AC square-wave, sawtooth-wave, and triangle-wave fields driven adiabatic quantum pumps in nanowire structures

Rui Zhu *, Xiao-Kang Zhang, and Xiaowen Chen

Department of Physics, South China University of Technology,

Guangzhou 510641, People's Republic of China

Abstract

A dc current can be pumped through a nanostructure by two out-of-phase ac driving fields. In this approach, we explore the pumped current properties driven by square-wave, sawtooth-wave, and triangle-wave ac fields in nanowire structures by Fourier expansion. The theory can be applied to arbitrary driving fields. It is found that the pumped current varies with the phase difference as square-wave and sawtooth-wave functions, respectively, under corresponding driven fields. The sinusoidal relation governs in the pump driven by triangle-wave oscillation. Devices based on square-wave driven quantum pumps may have potential applications in digital information at nanoscale dimensions.

PACS numbers: 73.63.-b, 05.60.Gg, 84.30.Sk

* Corresponding author. Electronic address: rzhu@scut.edu.cn

I. INTRODUCTION

Quantum pumping is a transport mechanism which induces dc charge and spin currents in a nano-scale conductor in the absence of a bias voltage by means of a time-dependent control of some system parameters. Research on quantum pumping has attracted heated interest since its experimental realization in an open quantum dot[1–32]. Harmonic-force-driven pumping properties in various nano-scale structures were investigated such as the magnetic-barrier-modulated two dimensional electron gas[4], mesoscopic one-dimensional wire[6,22], quantum-dot structures[5,11,12,28,32,33], mesoscopic rings with Aharonov-Casher and Aharonov-Bohm effect[7], magnetic tunnel junctions[10], chains of tunnel-coupled metallic islands[25], the nanoscale helical wire[26],the Tomonaga-Luttinger liquid[24], and garphene-based devices[20,21]. Recently, an ac-dc voltage probe to quantum driven systems was demonstrated and the local current profile was predicted[34]. Theory and experiments demonstrate that the harmonically-driven dc current produced at zero bias is sinusoidal in the phase difference between the two ac voltages in the adiabatic and weak pumping regime.

Recently, symmetries and transport properties of quantum pumps with biharmonic driving were investigated by several authors[31]. Keldysh non-equilibrium Green's function and the scattering-matrix method can be used to derive the pumped current in certain cases. However, quantum pumping driven by arbitrary fields is less investigated and that driven by fields with sharp fall and increase such as the square wave and sawtooth wave is beyond former approach. The square wave, sawtooth wave, and triangle wave are three typical non-sinusoidal waveforms. The square wave is widely used in electronics and signal processing, such as timing references or "clock signals". The sawtooth wave is one of the best waveforms to use for synthesizing musical sounds. Their significance in signal processing prompted our exploration of the quantum-pumping properties driven by two out-of-phase square-wave, sawtooth-wave, and triangle-wave ac fields and seeking the potential applications. Relevant theory can be extended to arbitrary-field-driven quantum pumps.

II. THEORETICAL FORMULATION

The square wave is a kind of non-sinusoidal waveform. Using Fourier expansion we can write an ideal square wave as an infinite series of the form

$$x_{Square}\left(\omega t\right)=\sum_{k=1}^{\infty}\frac{\sin\left[\left(2k-1\right)\omega t\right]}{\left(2k-1\right)}, \tag{1}$$

with the angular frequency of ω and the amplitude of $\pi/4$ (see the inset of Fig. 1). We consider the response of a mesoscopic phase-coherent sample to two slowly oscillating square-wave external fields $X_j(t)$ (gate potential, magnetic flux, etc.)[3], which can be expressed as

$$\begin{aligned} X_j\left(t\right) &= X_{0,j}+\tfrac{X_{\omega,j}}{2i}\sum_{k=1}^{\infty}\tfrac{\exp[i(2k-1)(\omega t-\varphi_j)]}{(2k-1)} \\ &\quad -\tfrac{X_{\omega,j}}{2i}\sum_{k=1}^{\infty}\tfrac{\exp[-i(2k-1)(\omega t-\varphi_j)]}{(2k-1)}, \\ j &= 1,2. \end{aligned} \tag{2}$$

$X_{0,j}$ and $X_{\omega,j}$ measure the static magnitude and the square-wave ac driving amplitude of the two parameters, respectively. The phase difference between the two drivers is defined as $\phi=\varphi_1-\varphi_2$. The mesoscopic conductor is connected to two reservoirs at zero bias. The scattering matrix $\hat{s}$ being a function of parameters $X_j(t)$ depends on time.

We suppose an adiabatic quantum pump, i.e., the external parameter changes so slowly that up to corrections of order $\hbar\omega/\gamma$ (γ measures the escape rate), we can apply an instant scattering description using the scattering matrix $\hat{s}\left(t\right)$ frozen at some time t. And we assume that the amplitude $X_{\omega,j}$ is small enough to keep only the terms linear in $X_{\omega,j}$ in an expansion of the scattering matrix[3]:

$$\hat{s}\left(t\right)\approx\hat{s}\left(X_{0,j}\right)+\sum_{k=1}^{\infty}\hat{s}_{-k\omega}e^{i(2k-1)\omega t}-\sum_{k=1}^{\infty}\hat{s}_{+k\omega}e^{-i(2k-1)\omega t}. \tag{3}$$

In the limit of small frequencies the amplitudes $\hat{s}_{\pm k\omega}$ can be expressed in terms of parametric derivatives of the on-shell scattering matrix $\hat{s}$,

$$\hat{s}_{\pm k\omega}=\sum_{j=1,2}\frac{X_{\omega,j}}{2i\left(2k-1\right)}e^{\pm i(2k-1)\varphi_j}\frac{\partial\hat{s}}{\partial X_j}. \tag{4}$$

The expansion, Eq. (3), includes sideband formation up to infinite orders, which implies that a scattered electron can absorb numerous energy quanta of $\hbar\omega$ before it leaves the scattering region. We would like to point out that square waves contain a wide range of

harmonics. Therefore the scattering matrix naturally includes high-order Fourier terms even in the linear-response limit. The conduction bandwidth of a semiconductor nanowire is of the order of meV within the non-dissipation regime[35] and an $\hbar\omega$ is of the order of 10^{-6} meV for an MHz frequency. The square-wave shape achieves acceptable approximation with 100 orders of harmonics present. The setting time is extremely small, while the Gibbs phenomenon is unavoidable. Thus formed sideband of even $100\hbar\omega$ constitutes a slight broadening in the conductance and the absorption/emission of a $100\hbar\omega$ quantum is physically justifiable. The effect of higher-order harmonics can be neglected.

The pumped current depends on the values of the scattering matrix within the energy interval of the order of $\max(k_BT, 100\hbar\omega)$ near the Fermi energy. In the low-temperature limit ($T \to 0$) and low-frequency limit ($\omega \to 0$), the scattering matrix can be assumed to be energy independent within a $100\hbar\omega \sim 10^{-4}$meV deviation as a driving frequency of the order of MHz is considered.

The mesoscopic scatterer is coupled to two reservoirs with the same temperatures T and electrochemical potentials μ. Electrons with the energy E entering the scatterer are described by the Fermi distribution function $f_0(E)$, which approximates a step function at a low temperature. Due to the interaction with an oscillating scatterer, an electron can absorb or emit energy quanta that changes the distribution function. A single transverse channel in one of the leads is considered. Applying the hypothesis of an instant scattering, the scattering matrix connecting the incoming and outgoing states can be written as

$$\hat{b}_\alpha(t) = \sum_\beta s_{\alpha\beta}(t)\,\hat{a}_\beta(t). \tag{5}$$

Here $s_{\alpha\beta}$ is an element of the scattering matrix $\hat{s}$; the time-dependent operator is $\hat{a}_\alpha(t) = \int dE \hat{a}_\alpha(E)\, e^{-iEt/\hbar}$, and the energy-dependent operator $\hat{a}_\alpha(E)$ annihilates particles with total energy E incident from the α lead into the scatter and obey the following anticommutation relations

$$\left[\hat{a}^\dagger_\alpha(E), \hat{a}_\beta(E')\right] = \delta_{\alpha\beta}\delta(E - E'). \tag{6}$$

Note that above expressions correspond to single- (transverse) channel leads and spinless electrons. For the case of many-channel leads each lead index (α, β, etc.) includes a transverse channel index and any repeating lead index implies implicitly a summation over all the transverse channels in the lead. Similarly an electron spin can be taken into account.

Using Eqs. (3) to (5) and after a Fourier transformation we obtain

$$\begin{aligned}\hat{b}_\alpha(E) = &\sum_\beta \hat{s}(X_{0,j})\,\hat{a}_\beta(E) \\ &+ \sum_\beta \sum_{k=1}^{\infty} \hat{s}_{-k\omega}\hat{a}_\beta[E+(2k-1)\hbar\omega] \\ &- \sum_\beta \sum_{k=1}^{\infty} \hat{s}_{+k\omega}\hat{a}_\beta[E-(2k-1)\hbar\omega].\end{aligned} \tag{7}$$

The distribution function for electrons leaving the scatterer through the lead α is $f_\alpha^{(out)}(E) = \left\langle \hat{b}_\alpha^\dagger(E)\,\hat{b}_\alpha(E)\right\rangle$, where $\langle\cdots\rangle$ means quantum-mechanical averaging. Substituting Eq. (7) we find

$$\begin{aligned}f_\alpha^{(out)}(E) = &\sum_\beta |\hat{s}(X_{0,j})|^2 f_0(E) \\ &+ \sum_\beta \sum_{k=1}^{\infty} |\hat{s}_{-k\omega}|^2 f_0[E+(2k-1)\hbar\omega] \\ &+ \sum_\beta \sum_{k=1}^{\infty} |\hat{s}_{+k\omega}|^2 f_0[E-(2k-1)\hbar\omega].\end{aligned} \tag{8}$$

The distribution function for outgoing carriers is a nonequilibrium distribution function generated by the nonstationary scatterer. The Fourier amplitudes of the scattering matrix $|\hat{s}_{-k\omega,\alpha\beta}|^2$ ($|\hat{s}_{+k\omega,\alpha\beta}|^2$) is the probability for an electron entering the scatterer through the lead β and leaving the scatterer through the lead α to emit (to absorb) an energy quantum of $\hbar k\omega$. $|\hat{s}(X_{0,j})|^2$ is the probability for the same scattering without the change of energy.

Using the distribution functions $f_0(E)$ for incoming electrons and $f_\alpha^{out}(E)$ for outgoing electrons, the pumped current measured at lead α reads

$$I_p = \frac{e}{2\pi\hbar}\int_0^\infty \left\langle \hat{b}_\alpha^\dagger(E)\,\hat{b}_\alpha(E)\right\rangle - \left\langle \hat{a}_\alpha^\dagger(E)\,\hat{a}_\alpha(E)\right\rangle dE. \tag{9}$$

Substituting Eqs. (8) and (4) into Eq. (9) we get

$$\begin{aligned}I_p &= \tfrac{ie\omega}{4\pi}\sum_\beta \sum_{k=1}^{\infty}\sum_{j_1,j_2} \tfrac{X_{\omega,j_1}X_{\omega,j_2}}{(2k-1)} \sin[(2k-1)(\varphi_{j_1}-\varphi_{j_2})]\,\tfrac{\partial \hat{s}^*_{\alpha\beta}}{\partial X_{j_1}}\tfrac{\partial \hat{s}_{\alpha\beta}}{\partial X_{j_2}} \\ &= \tfrac{ie\omega}{4\pi}\sum_\beta \sum_{j_1,j_2} X_{\omega,j_1}X_{\omega,j_2}\tfrac{\partial \hat{s}^*_{\alpha\beta}}{\partial X_{j_1}}\tfrac{\partial \hat{s}_{\alpha\beta}}{\partial X_{j_2}} x_{Square}(\varphi_{j_1}-\varphi_{j_2}).\end{aligned} \tag{10}$$

Quantum pumping properties driven by ac square-wave fields are demonstrated in Eq. (10). It can be directly seen that the pumped current varies with the phase difference of the two drivers in a square-wave pattern. The magnitude of the pumped current is modulated by the driving amplitude and the scattering matrix derivatives. The wave function of the pumped current is exactly square-shaped with all harmonics involved. Physically, in the Fourier series, energy quanta of $\hbar k\omega$ emission (absorption) processes with k ranging many

orders determine the pumped current. High-order Fourier terms diminish due to a large denominator produced in the Fourier expansion. Numerical results will show that expanding to the 100th harmonic generates a square-wave shape with extremely small ringing effect and higher-order harmonics can be neglected. The relation between the pumped current and the ac driving amplitude $X_{\omega,j}$ is linear in the adiabatic weak-modulation limit. The linear dependence of the pumped current on the oscillation frequency holds valid as the adiabatic approximation is considered.

Following the same theory and similar derivation, the pumped current driven by two out-of-phase sawtooth-wave and triangle-wave fields can be obtained as in Eqs. (11) and (12), respectively.

$$\begin{aligned} I_p &= \tfrac{ie\omega}{4\pi} \sum_{\beta} \sum_{k=1}^{\infty} \sum_{j_1,j_2} \tfrac{X_{\omega,j_1} X_{\omega,j_2}}{k} \sin\left[k\left(\varphi_{j_1} - \varphi_{j_2}\right)\right] \tfrac{\partial \hat{s}^*_{\alpha\beta}}{\partial X_{j_1}} \tfrac{\partial \hat{s}_{\alpha\beta}}{\partial X_{j_2}} \\ &= \tfrac{ie\omega}{4\pi} \sum_{\beta} \sum_{j_1,j_2} X_{\omega,j_1} X_{\omega,j_2} \tfrac{\partial \hat{s}^*_{\alpha\beta}}{\partial X_{j_1}} \tfrac{\partial \hat{s}_{\alpha\beta}}{\partial X_{j_2}} x_{Sawtooth}\left(\varphi_{j_1} - \varphi_{j_2}\right), \end{aligned} \tag{11}$$

$$I_p = \frac{ie\omega}{4\pi} \sum_{\beta} \sum_{k=1}^{\infty} \sum_{j_1,j_2} \frac{X_{\omega,j_1} X_{\omega,j_2}}{(2k-1)^3} \sin\left[(2k-1)\left(\varphi_{j_1} - \varphi_{j_2}\right)\right] \frac{\partial \hat{s}^*_{\alpha\beta}}{\partial X_{j_1}} \frac{\partial \hat{s}_{\alpha\beta}}{\partial X_{j_2}}. \tag{12}$$

In Eq. (11), $x_{Sawtooth}$ is the function of a sawtooth wave analogous to Eq. (1). It can be seen from Eqs. (10) and (11) that in our approach the Fourier expansion in the signal function can be converted back to the original wave form as a function of the phase difference in the pumped current for square-wave and sawtooth-wave signals. For triangle-wave signals, the higher harmonics roll off much faster than in square and sawtooth waves (proportional to the inverse square of the harmonic number as opposed to just the inverse). In pumping mechanisms, that attenuation is magnified with each harmonic term in the pumped current proportional to the inverse cubic of the harmonic number and original triangle-wave shape can not be reproduced.

It is worth mentioning that former scattering approach[2] to quantum pumping gives a general formula of the pumped current for arbitrary parameter variation pattern. However, for square- and sawtooth-wave modulation, sharp fall and increase presents in the parameter variation. Without Fourier series expansion, direct parameter derivatives diverge. If we use the Fourier series, numerical solution of the area integral in the parameter space becomes extremely difficult[36]. In the Keldysh formalism[31,32], the Green's function is difficult to be derived from the equation of motion with the square-wave time-dependent potential

modulating the Hamiltonian. The problem is numerically solvable by our approach and the numerical efficiency is markedly improved .

In the next section, numerical results of the pumped current in a two-oscillating-potential-barrier modulated nanowire are presented.

III. NUMERICAL RESULTS AND INTERPRETATIONS

We consider a nanowire modulated by two gate potential barriers with equal width $L = 20$ Å separated by a $2L = 40$ Å width well. The electrochemical potential of the two reservoirs μ is set to be 60 meV according to the resonant level within the double-barrier structure. The two oscillating parameters in Eq. (2) correspond to the two ac driven potential gates. We set the static magnitude of the two gate potentials $U_{0,1} = U_{0,2} = U_0 = 100$ meV and the ac driving amplitude of the modulations equal with $U_{\omega,1} = U_{\omega,2} = U_\omega$.

Figs. 1, 2, and 3 present numerical results of the dc current pumped by square-wave, sawtooth-wave, and triangle-wave drivers, respectively. Corresponding driving signals are shown in insets. Numerical calculation takes into account the foremost 100 orders of the Fourier series. As shown in Fig. 1, the pumped current varies with the phase difference between the two drivers in a square-wave pattern when the driving signal is a square wave, which is a direct result of former analysis [see Eq. (10) and previous derivation]. Phase difference has a modulation to the time dependence of the driving forces. The pumped current varies with the phase difference in a sinusoidal pattern when the driving field is a sinusoidal wave as a function of time. When higher-order harmonics are present, the effect of the phase difference is similar to the sinusoidal harmonic when their strength depends linearly-inversely on the order number. This behavior is also demonstrated in the sawtooth wave case, as shown in Fig. 2 and formulized in Eq. (11). Different from the square-wave and sawtooth-wave fields, the pumped current driven by triangle varies with the phase difference of the two ac gate voltages in a sinusoidal pattern as the higher harmonics roll off much faster [see Fig. 3 and Eq. (12)].

Our theory can be extended to arbitrary-field-driven quantum pumps. When the strength of all orders of the Fourier expansion is proportional to the inverse of the harmonic number, the signal pattern as a variation of the time can be reproduced in the pumped current as a variation of the phase difference. In other cases, the reproduction would not occur. It can

also be inferred from our theory that the variation of the pumped current as a function of the phase difference would deviate from the wave pattern even for sinusoidal, square-wave, and sawtooth-wave ac fields when the driving force is strong beyond the linear response limit[30].

In digital information technology, square waves and sawtooth waves are two types of widely used digital signals. Classic oscilloscopes and phase detectors are usually based on LC circuits. In our approach, the characteristics of the pumped current bear information of both the wave pattern and wave phase of the input ac signals. Potential development of the currently smallest quantum oscilloscopes and phase detectors can be foreseen from the theoretical approach.

IV. CONCLUSIONS

Two out-of phase harmonic ac fields driven quantum pumps have a sinusoidal dependence of the pumped current on the phase difference of the two drivers. We developed the scattering-matrix method to explore the pumping properties driven by square-wave, sawtooth-wave, and triangle-wave ac fields by harmonic expansion of the time-dependent signals. It is demonstrated that the pumped current varies with the phase difference of the two ac fields as a square-wave and sawtooth-wave pattern driven by corresponding wave signals. The theory can be extended to arbitrary field driven quantum pumps, which infers that the signal time-dependent pattern can be reproduced in the phase dependent pumped current in certain cases. The wave pattern and phase information of the input signal carried by the pumped current in the proposed configuration suggests its potential applications.

V. ACKNOWLEDGEMENTS

This project was supported by the National Natural Science Foundation of China (No. 11004063), the Fundamental Research Funds for the Central Universities, SCUT (No. 2009ZM0299), the Nature Science Foundation of SCUT (No. x2lxE5090410) and the Graduate Course Construction Project of SCUT (No. yjzk2009001).

[1] M. Switkes, C. M. Marcus, K. Campman, and A. C. Gossard, Science **283**, 1905 (1999).

[2] P. W. Brouwer, Phys. Rev. B **58**, R10135 (1998). M. Büttiker, H. Thomas, and A. Prêtre, Z. Phys. B **94**, 133 (1994); Phys. Rev. Lett. **70**, 4114 (1993).

[3] M. Moskalets and M. Büttiker, Phys. Rev. B **66**, 035306 (2002).

[4] R. Benjamin and C. Benjamin, Phys. Rev. B **69**, 085318 (2004).

[5] H. C. Park and K. H. Ahn, Phys. Rev. Lett. **101**, 116804 (2008).

[6] P. Devillard, V. Gasparian, and T. Martin, Phys. Rev. B **78**, 085130 (2008).

[7] R. Citro and F. Romeo, Phys. Rev. B **73**, 233304 (2006).

[8] M. Moskalets and M. Büttiker, Phys. Rev. B **72**, 035324 (2005).

[9] M. Moskalets and M. Büttiker, Phys. Rev. B **75**, 035315 (2007).

[10] F. Romeoa and R. Citro, Eur. Phys. J. B **50**, 483 (2006).

[11] J. Splettstoesser, M. Governale and J. König, Phys. Rev. B **77**, 195320 (2008).

[12] M. Strass, P. Hänggi, and S. Kohler, Phys. Rev. Lett. **95**, 130601 (2005).

[13] J.E. Avron, A. Elgart, G.M. Graf, and L. Sadun, Phys. Rev. Lett. **87**, 236601 (2001).

[14] B. G. Wang, J. Wang, and H. Guo, Phys. Rev. B **65**, 073306 (2002).

[15] B. G. Wang and J. Wang, Phys. Rev. B. **66**, 125310 (2002).

[16] B. G. Wang, J. Wang, and H. Guo, Phys. Rev. B **68**, 155326 (2003).

[17] L. Arrachea, Phys. Rev. B **72**, 125349 (2005).

[18] Y. Tserkovnyak, A. Brataas, G. E. W. Bauer, and B. I. Halperin, Rev. Mod. Phys. **77**, 1375 (2005).

[19] D. C. Ralph and M. D. Stiles, J. Magn. Magn. Mater. **320**, 1190 (2008).

[20] R. Zhu and H. Chen, Appl. Phys. Lett. **95**, 122111 (2009).

[21] E. Prada, P. San-Jose, and H. Schomerus, Phys. Rev. B **80**, 245414 (2009).

[22] A. Agarwal and D. Sen, J. Phys.: Condens. Matter **19**, 046205 (2007).

[23] L. E. F. Foa Torres, Phys. Rev. B **72**, 245339 (2005).

[24] A. Agarwal and D. Sen, Phys. Rev. B **76**, 235316 (2007).

[25] N. Winkler, M. Governale, and J. König, Phys. Rev. B **79**, 235309 (2009).

[26] X. L. Qi and S. C. Zhang, Phys. Rev. B **79**, 235442 (2009).

[27] S. J. Wright, M. D. Blumenthal, M. Pepper, D. Anderson, G. A. C. Jones, C. A. Nicoll, and D.

A. Ritchie, Phys. Rev. B **80**, 113303 (2009).

[28] F. Romeo and R. Citro, Phys. Rev. B **80**, 165311 (2009).

[29] M. Moskalets and M. Büttiker, Phys. Rev. B **66**, 205320 (2002).

[30] R. Zhu, Chin. Phys. B, **19**, (2010) (in press).

[31] L. Arrachea, Physica B **398**, 450 (2007).

[32] K. Hattori, Phys. Rev. B **78**, 155321 (2008).

[33] L. P. Kouwenhoven, A. T. Johnson, N. C. van der Vaart, C. J. P. M. Harmans, and C. T. Foxon, Phys. Rev. Lett. **67**, 1626 (1991).

[34] F. Foieri and L. Arrachea, Phys. Rev. B **82**, 125434 (2010).

[35] L. Stella, G. E. Santoro, M. Fabrizio, and E. Tosatti, Surface Science **566C568**, 430 (2004).

[36] By Monte Carlo algorithms that numerical integration may become viable if additional programming efforts are made.

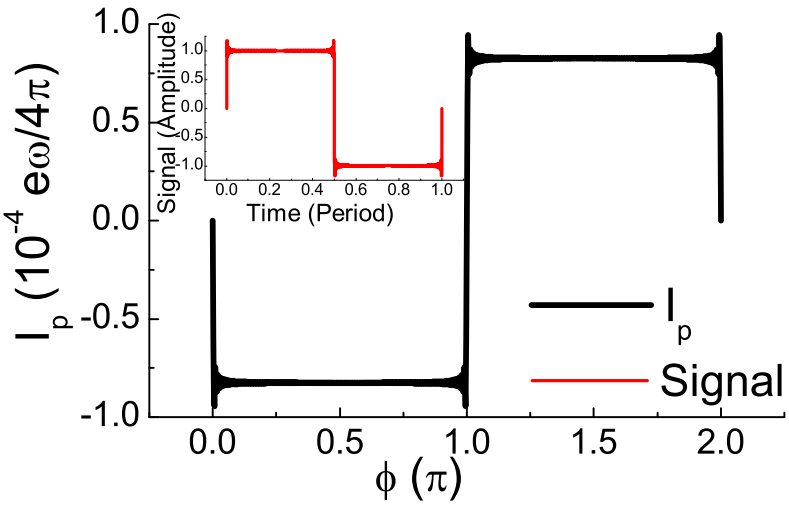

FIG. 1: Pumped current driven by ac square-wave fields as a function of the phase difference between the two modulations. Inset is the time-variation of the wave signal. The foremost 100 harmonics are considered in numerical treatment.

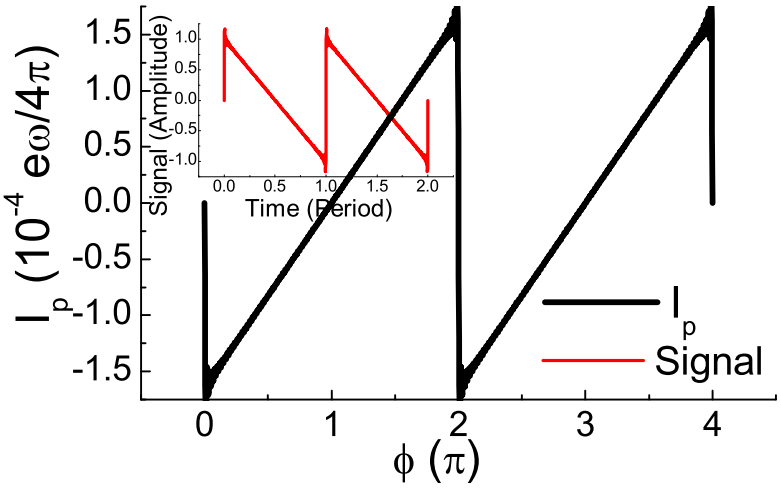

FIG. 2: Pumped current driven by ac sawtooth-wave fields as a function of the phase difference between the two modulations. Inset is the time-variation of the wave signal. The foremost 100 harmonics are considered in numerical treatment.

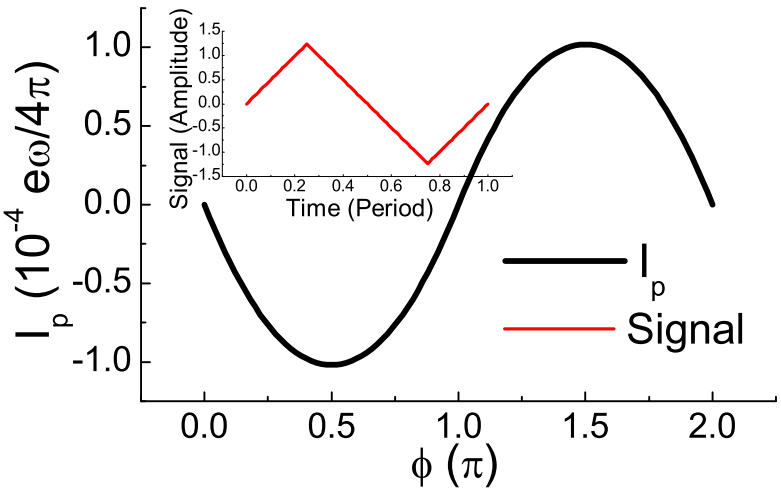

FIG. 3: Pumped current driven by ac triangle-wave fields as a function of the phase difference between the two modulations. Inset is the time-variation of the wave signal. The foremost 100 harmonics are considered in numerical treatment.